The Climate Change Impact on Power Grid Transmission Capacity

Sergio Daniel Montana Salas, Andrea Michiorri

The Climate Change Impact on Power Grid Transmission Planning

Montaña-Salas Sergio, Michiorri Andrea

October 25, 2024

Abstract

Proposing practical solutions to mitigate climate change effects on the electrical power system requires a comprehensive understanding and quantification. By conducting an assessment at high grid resolution, this article explores the impact of climate on transmission network capacity, employing established thermal models and a regional expansion plan. The results indicate average reductions of 1.53%, 2.3%, and 0.2% for overhead lines, power transformers, and underground cables, respectively. We propose a quasi-Dynamic Thermal Rating method to counter these effects, estimating maximum capacity. This approach enhances component capacity by an average of up to 35% during winter at the power transformers and up to 14% during nighttime hours for overhead lines. This solution constitutes a viable alternative for electricity operators to address the dilemma between the necessity of reducing the failure rate/decrease in capacity and the imperative need for new investments in transmission assets.

Climate Change, Dynamic Thermal Rating , Power Systems Planning, Power transmission.

1 Introduction

Climate change projections estimate an average atmospheric temperature increase of 2-4^{o}C until the end of the century [1, 2]. This will directly and negatively impact the electric power system, affecting transmission capacity, generation, demand, and congestion.

Regarding transmission, which is the main focus of this study, the current carrying capacity of Overhead Lines (OHL), Power Transformers (PT), and Underground Cables (UGC) is determined, among other factors, by their ability to dissipate joule losses into the external environment. In turn, this depends on ambient temperature: the lower the external temperature, the higher the transmission capacity, and vice versa. For instance, in the United States, the impact of global warming is anticipated to cause a reduction in OHL capacity within the range of 1.9% to 5.8% [3].

In reference to power generation, higher temperatures lead to a reduction in production capacity: on the one hand, a higher ambient temperature increases the sink temperature in thermodynamic cycles, reducing overall conversion efficiency. On the other hand, it reduces air density, which, in turn, reduces the mass flow intake of fossil fuel generators. Furthermore, factors such as water discharge temperatures and diminishing water flows are anticipated to impact over 80% of the world's thermal power plants due to drought and shifting seasonal patterns, as detailed in [4].

Regarding power demand, this tends to grow with higher ambient temperature due to load thermosensitivity driven by air conditioning. This is, in turn, accentuated by the growing penetration of air cooling in power systems, including in developing countries. In [5], the expected annual demand variation in different scenarios ranges from -2.7% to 5.7% on average and is further exacerbated during heat waves, culminating in an increase of up to 21% [6].

The combination of lower transmission capacities, lower generation, and higher load can increase the likelihood of congestion in the transmission and distribution infrastructure. This leads to inefficiency and spikes in local power prices, exacerbating current trends which, for example, resulted in a cost of roughly $4.8 billion in 2016, as the U.S.

Department of Energy (DOE) reported in 2018 [7].

Among the solutions proposed to alleviate network congestion problems, Dynamic Thermal Rating (DTR) [8–11] is actively being deployed on critical lines. This technology aims to identify the real-time current carrying capacity of network components, which is generally higher than its Static Thermal Rating (STR). On the one hand, this value is strongly weather-dependent; on the other, DTR allows the removal of network congestions and associated curtailments and delays and can remove network reinforcements whilst improving reliability.

Various studies have incorporated DTR into power system expansion plans [12, 13] and highlighted its importance in RES integration and penetration [14–18]. These studies employ control and sensing devices [19, 20] or data-driven probabilistic methods to calculate the rating of OHL [21]. All these studies yield generalized findings on the efficacy of DTR, among which the following can be emphasized: a) Decreased system congestion costs due to less generator re-dispatching. b) Reduction or postponement of investments required for reinforcing or expanding existing assets. c) Grid operational flexibility to enhance facilitated integration of RES.

In this study, we leverage historical and projected meteorological variables on the power system component's location at different geographical points. Through this data, we calculate the maximum current that the system can carry at any point in time without any section's temperature surpassing the predefined maximum threshold, employing the DTR methodology. By doing so, we emphasize the significant potential of DTR in enhancing power system flexibility. To reinforce this assertion, we analyze power system planning within the Generation and Transmission Expansion Plan (G&TEP) framework using a tool for modeling hybrid power systems.

This is made possible by the availability of widely accepted component thermal models [22–24], open energy data models [25] and quantitative climatic projections such as the Representative Concentration Pathways (RCPs) [26] and Shared Socioeconomic Pathways (SSPs) [27], which constitute a valuable toolset for assessing regional climate changes and their specific impacts on the energy sector.

In summary, although research on the impact of climate change on the energy system is becoming more mature, the above literature review identifies several notable research gaps, highlighting areas where further research and analysis are necessary. Among them :

1) Previous research on this topic has primarily focused on the impact of generation production [15, 28–30] and load [5]. When network aspects were taken into account, only OHL were considered [3].

2) To the authors' knowledge, the impact of climate change on long-term in power grid transmission, including dynamic thermal rating in OHL [3, 10], UGL [31, 32], and PT [15, 18, 33], has yet to be thoroughly examined. Most studies have focused on short and medium-term analysis when applying DTR [32, 34].

3) In these works, the problem and its consequences are clearly defined and quantified. However, solutions are not suggested, apart from relying on traditional network reinforcements or smart grid approaches. Limited research has focused on developing stable dynamic methods and probabilistic approaches for network operational planning over extended periods for OHL [21, 34, 35], PT, and UGC.

In light of this, this research aims at providing the following main contributions :

Quantify the impact of climate change on power system transmission capacity for OHL, PT, and UGL, considering both historical reanalysis and future climatic projections datasets. This quantification is done in terms of transmission capacity (in MVA) and costs for G&TEP.

It also proposes quasi-Dynamic Thermal Rating (qDTR) as the primary solution to recover lost transmission capacity, facilitating the connection of renewable resources and reducing network costs.

2 Methodology

2.1 Overview

We develop a procedure to quantify the impact of climate change on power grid transmission capacity. This method is described in Fig. 1 and can be divided into two steps:

Firstly, DTR and qDTR are estimated for OHL, PT, and UGC [36] using thermal models of the components and weather data from historical re-

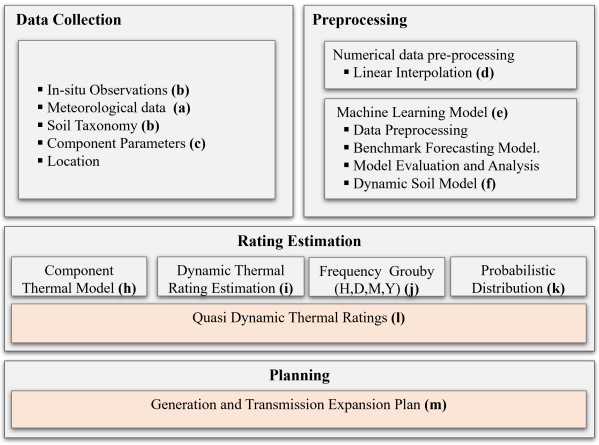

Figure 1: Visual representation of the procedure used in this study.

analysis and climatic projections. This allows us to quantify the variation in transmission capacity due to climate change.

Secondly, a G&TEP is calculated with a horizon of 2050, using transmission capacities calculated with historical weather reanalysis and RCPs projections for STR, and qDTR. This allows us to quantify the impact of climate change on transmission capacity, which was calculated in the previous step.

2.2 Data

The data used in this study can be divided into two broad categories: (c) component data (static) and (a) environment data (static and dynamic). Historical meteorological conditions in Europe for the period 1970-2020 are obtained from ERA reanalysis [2], whilst climatic projections for the period 2020-2070 are obtained from the Copernicus Climate Change Service (C3S) [1]. Additional (b) soil properties for underground cable rating calculations are obtained from [37, 38]. A list of the parameters used and their source is reported in Table. 1. Component parameters, relative to the most popular elements, are obtained from the existing literature or data sheets provided by the main manufacturers, such as [39] for OHL, [40] for UGC, and [41] for PT.

Table 1: Summary of data and sources. a:ERA [1, 2], b:ISMN [37], c:ESDAC [38].

Variable	Units	Source
Meteorological		
Temp. Air at 2 m (θ_a)	K	A
Total precipitation (P_t)	mm	A
Net surface solar radiation (S_r)	Jm^{-2}	A
u - v - wind at 10 m (W_s)	ms^{-1}	A
Soil Proprieties		
Silt ($S_{silt_{\%}}$)	%	C
Sand ($S_{sand_{\%}}$)	%	C
Clay ($S_{clay_{\%}}$)	%	C
Organic ($S_{org_{\%}}$)	%	C
Texture Composition (S_{text})	-	C
Bulk (S_{bulk})	kgm^{-3}	C
Soil Measurements		
Temperature (θ)	K	B
Moisture (ψ)	%	B

2.3 Preprocessing

The raw data described are pre-processed as follows: (d) time series are uniformed by linear interpolation to a common time step of 1h. When a specific coordinate is required, parameters are interpolated linearly from the four nearest available grid points. (f) soil temperature ($\hat{\theta}_s$) and soil moisture ($\hat{\psi}$) are calculated with a daily resolution in a depth range between 0.8 and 1.2 meters based on hourly-recorded input data, using a dedicated machine-learning-based model (e) for each coordinate (0.25°), described by the authors in [36]. This is necessary since the available values from [1] are either not obtainable at the typical UGC burial depth (1-5m, in the case of soil temperature) or absent (in the case of soil moisture).

2.4 Rating estimation

The estimation of ratings starts with the use of (h) component thermal models based on the thermal balance between the heat generated by the Joule effect I^2R and the heat dissipated in the environment by convection or conductivity Q_c, radiation Q_r and the solar heat gain Q_s. This is shown in Eq. 1. From this fundamental equation is declined

as described below for each different component.

$$I^2R + Q_s = Q_r + Q_c \tag{1}$$

As mentioned above, the OHL thermal is calculated using the heat balance equation and applying the model outlined in [24]. The focus for calculating the conductor's rating can be outlined as follows:

$$I = \left[\frac{(\beta Q_r(\theta_a) + \gamma Q_c(\theta_a, W_s) - \alpha Q_s(S_r)}{R(\theta_a)}\right]^{(0.5)} \tag{2}$$

Where wind speed (W_s) poses the most challenging conditions for overhead lines as reported in [19] , coupled with factors like air temperature θ_a and solar radiation S_r.

Regarding underground cables, in accordance with the standard procedures for quantifying the ampacity of buried UGC, the thermo-electric model described in [23] is used for this component. According to this standard, the capacity, with the influence of a dry area formation, is calculated per day as follows.

The above equation focuses on the critical temperature of the boundary between the wet and dry zones ${}_{\Delta}\theta_x$ and the ratio between the thermal resistivity of the dry and wet zones of the back-fill soil v. With high dependence on variable factors such as ambient temperature, moisture, and precipitation, the other parameters such as λ_{1-2}, C, R, T_{1-3}, W_d obey the cable construction. These parameters can be determined and calculated according to [23, 42], guides, and suggestions.

Finally, several models are available to estimate the thermal state of loaded power oil-immersed transformers' capacity. Due to its broad recognition, this study adopts the widely accepted and straightforward IEC 60076-7 [22] loading guide. It is modified to incorporate the solar radiation factor on the component as described in [43]. PT rating is limited by the HST θ_h (°C), depending on ambient temperature θ_a (°C) and the hot-spot gradient rise of temperature within the transformer $\Delta\theta_h$ and it is calculated in Eq. 4. The Top-oil temperature θ_o (°C) with a cold start state assumptions can be calculated in Eq. 5.

$$I = \sqrt{\frac{{}_{\Delta}\theta - W_d\left[0.5T_1 + n\left(T_{2+3} + vT_4\right)\right] + (v-1){}_{\Delta}\theta_x}{R\left[T_1 + n\left(1+\lambda_1\right)T_2 + n\left(1+\lambda_{1+2}\right)\left(T_2 + vT_4\right)\right]}} \tag{3}$$

$$\Theta_o = \left[\frac{1+K^2R}{1+R} + \frac{S_r}{P_{LL}+PNL}\right]^x (\Delta\theta_{or}) + \theta_a \tag{4}$$

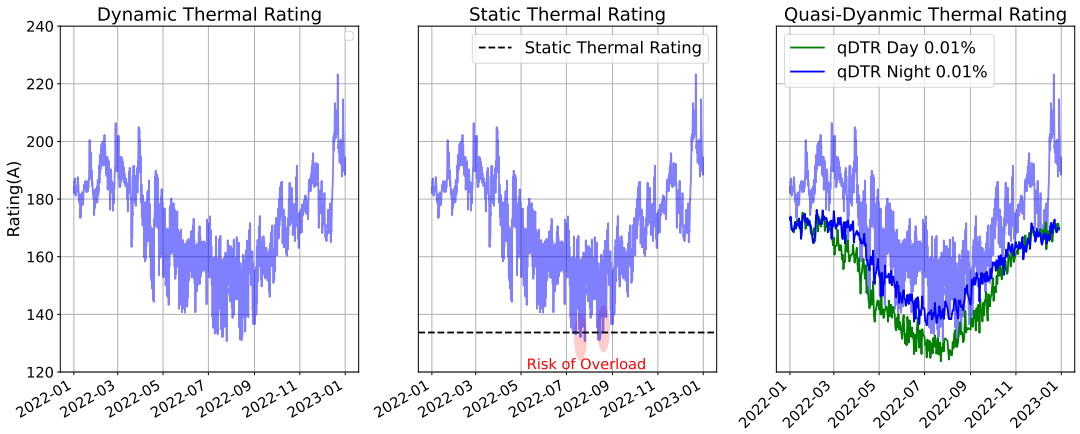

Figure 2: Conceptual illustrations of power system component rating capacities can be categorized into different methods. For DTR, a thermal model is utilized to compute the maximum capacity, taking into account real-time variables. Contrastingly, for STRs, a fixed value is applied throughout the year as a constrained capacity limit, without considering changing conditions. qDTR calculates a 0.1% overload risk over the lower tail values of DTR across a 50-year time horizon. Notably, cooler forced temperatures and lower irradiation levels increase the capacity during the winter season and nighttime hours.

$$\Theta_h = \theta_o + (\Delta\theta_{h2} - \Delta\theta_{h1}) \quad (5)$$

$$k_{21} \cdot K^y (\Delta\theta_{hr}) = \Delta\theta_{h1} \quad (6)$$

$$(k_{21} - 1) \cdot K^y (\Delta\theta_{hr}) = \Delta\theta_{h2} \quad (7)$$

Here, $\Delta\theta_{or}$ (°C) denotes the steady-state temperature rise at rated losses; x represents the exponent associated with oil temperature rise due to total losses, while R signifies the ratio of load losses at rated current to no-load losses at rated voltage. The hot-spot temperature (HST) serves as the pivotal limiting parameter for the rating, and it is instrumental in computing the load factor K (per unit) per iteration. This load factor is defined as the ratio of load current to rated current. Finally, the solar power is normalized into the load P_{LL} and the no-load losses P_{NL} in Eq. 4.

The state of the art thermal models for OHL [24], UGC [23], and PT [22] are used to compute the DTR (i) for each power component at each coordinate and each hourly time step available in the datasets [1, 2].

At this point, (j) the simulated historical or future DTRs are grouped by time interval (yearly, monthly, monthly/hourly). For each group, a power law function is fitted to the lowest tail of the distribution (k). Finally, an accepted risk for thermal overload is chosen, $x = 0.1\%$ in this work, and the qDTR in terms of current intensity I are calculated (l) as in Eq. 8, and conceptually illustrated in Fig. 2.

$$I(x) = Ax^{\alpha} \quad (8)$$

2.5 Planning

The financial impacts resulting from the reduction in DTR due to climate change are assessed through a series of G&TEP using [44] and CO_2 budgets for the RCPs from [45–51]. These studies rely on the use of yearly STRs and monthly/hourly DTRs (mhDTR), equivalent to 288 DTRs calculated for each month/hour combination. Several comparisons are carried out:

1) G&TEP are carried out using $\mathrm{STR_H}$ calculated on a historical reanalysis and $\mathrm{qDTR_{RCP}}$ on the three climatic projections. The comparison shows the error incurred when not considering the impact of climate change on transmission capacity.

2) G&TEP are carried out using $\mathrm{STR_H}$ and monthly/hourly $\mathrm{qDTR_H}$ calculated from historical reanalysis. The comparison shows the benefits of using frequently changing qDTR to recover the lost transmission capacity.

The G&TEP is carried out using the library PyPSA [25], modified in order to accept variable ratings. This solution allows us to rely on a widely used model to test the impact of the hypotheses and produce solid results. Nevertheless, this presents several limitations, notably the fact that the network run in PyPSA Europe is made of zones and their interconnections, whilst a real network has a far higher number of nodes and, more importantly, lines.

3 Results

This study applies qDTR to estimate the maximum allowable current carrying capacity of power transmission components using historical ($\mathrm{qDTR_H}$, from 1970 to 2022) and future weather projections for Europe ($\mathrm{qDTR_{RCPx}}$, where x represents the RCPs scenario of future greenhouse gas emissions evaluated from 2023 to 2070).

The first objective of this study is to analyze climate change's impact on components' transmission capacity. This can be seen in Table 2, where STR calculated with future climate projections are, on average, lower than when calculated with historical reanalysis. PT are the most affected component, with average rating reductions up to -3.7%, whilst UGC are the least affected, with average reductions in the region of -0.2% due to the lower thermal variability of the soil. For OHL, the average rating reduction is -0.9%. The spatial variability of these variations can be seen in Fig. 4 and 3, where some regions, such as the southern Iberian Peninsula or mountainous regions where reductions can arrive at -5.5%.

After this, climate change's impact on network costs is analyzed. This can be seen in Table 3, where cost variations are, in general, very small, with slight cost reductions in the case of $RCP_{4.5}$ and $RCP_{8.5}$ and slight cost increases in the case of $RCP_{2.6}$. It is believed that this is because constraints are seldom reached, and the network can

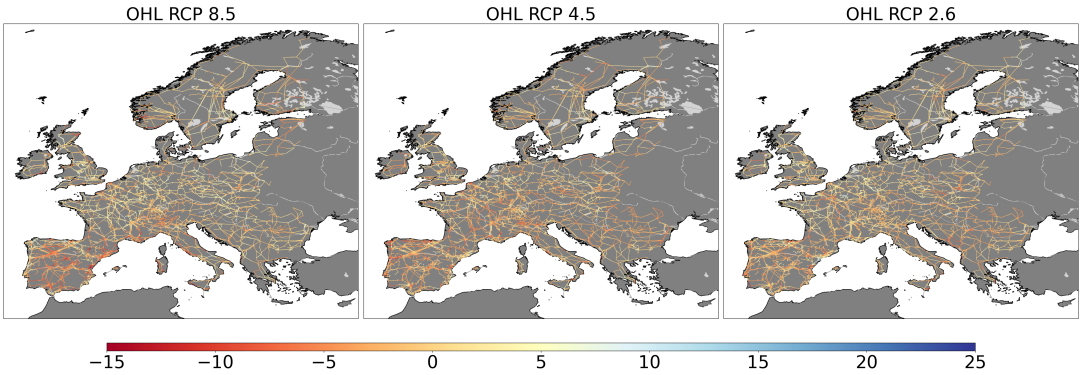

Figure 3: Climate impacts on transmission capacity, difference in capacity for qDTR in the month of June under the average RCP 2,6, 4.5 and 8.5 scenario for OHL.

easily rearrange its loads and production patterns to overcome them.

The impact of using qDTR instead of STR on transmission capacity is then studied. By maximising transmission limits always except in the central hours of the day, this approach allows to increase the average transmission capacity in Europe by 14.2%, 17.4%, and 3.7% for OHL, PT and UGC.

It is then tested how the new transmission capacity obtained by using qDTR instead of STR impact on network costs. Results are presented in Table 3, where costs increase slightly in the European use case and fall slightly in the French use case, except for $RCP_{4.5}$ in Europe, where costs increase considerably up to 6.5%. The next sections show firstly the increased transmission capacity allowed by qDTR, then the impact of climate change on network transmission capacity calculated by qDTR and finally the effect of climate change on network planning.

3.1 Impact of climate change on network transmission capacity

When qDTR are calculated using projections for the next decades instead of weather data relative to past years, the effect of a temperature rise predicted by climatic projections becomes apparent. Table 2 reports the average and extreme values for the difference in transmission capacity calculated using historical and expected future weather data. In all three scenarios, transmission capacity is expected to drop. Transformers are the component with the highest variation (from -1.0% to -2.3%), followed by OHL (from - 0.4% to -1.53%) and UGC (from -0.1% to -0.2%). This is explained by the fact that the OHL rating is mainly influenced by air temperature and wind speed, whilst the PT rating is only influenced by air temperature. Often the hottest hours are also characterized by not null wind speeds, reducing the derating effect of temperature. For UGC, the much narrower temperature variation of the soil prevents large rating drops. The worst simulated cases show a maximum reduction of -3.9%, -5.1%, and -1% for the ratings of OHL, PT, and UGC, respectively.

Fig. 4 shows the spatial distribution of the rating variations summarized in Table 2. The spatial variation of average transmission capacity for the three components is reported above.

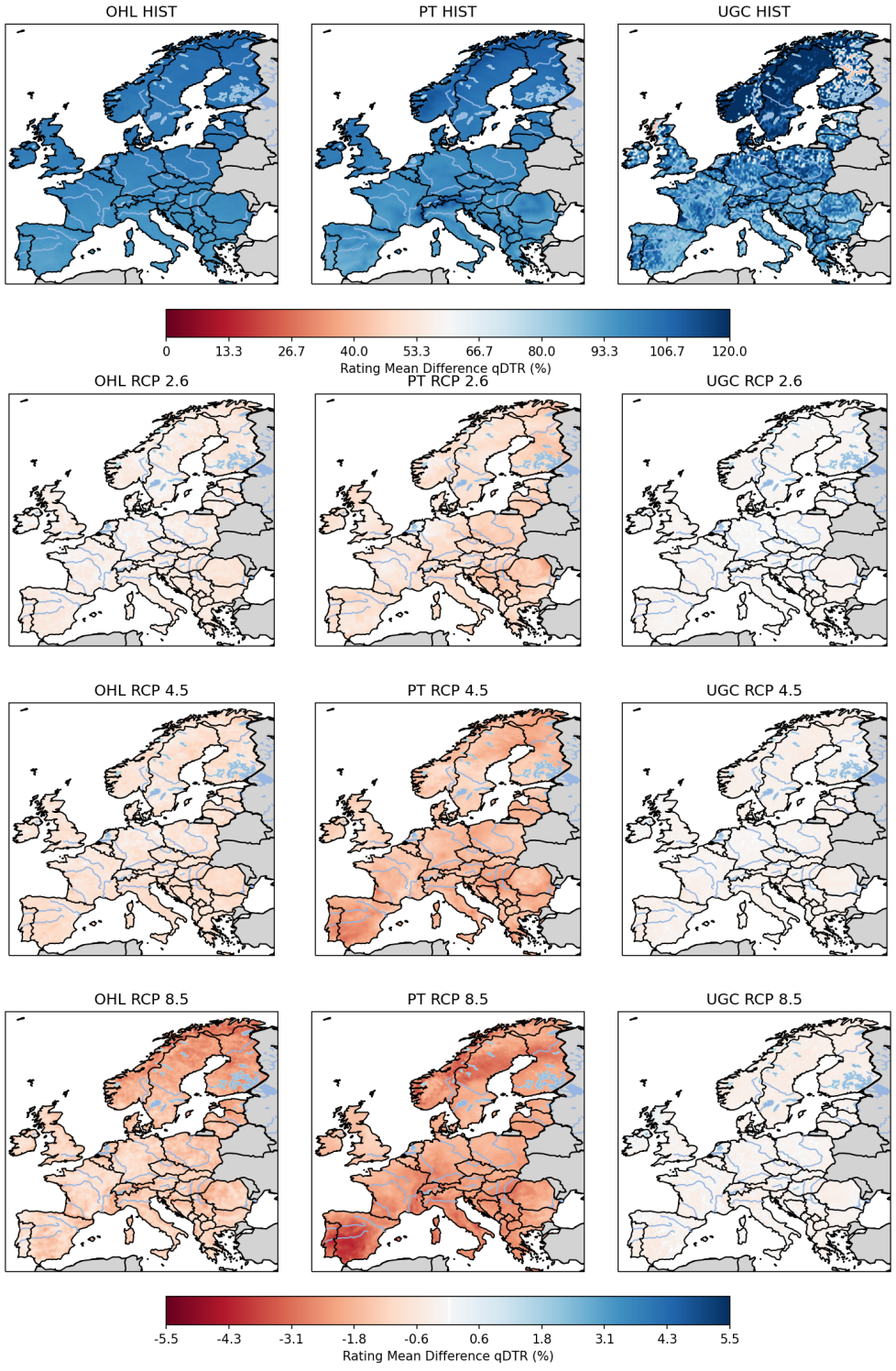

Figure 4: Geographical distribution of the mean qDTR difference at the country level over fifty years for the RCPs and the historical reanalysis. This is performed for the main power components (OHL - PT and UGC). The first row reflects the difference in the variation of the historical average for the region, and the subsequent rows illustrate the variation in the average for each RCP.

Table 2: Variation for the three scenarios concerning historical values for qDTR for the European region.

Description	Component		
	OHL	PT	UGC
$\Delta_{\%}(\mathbf{qDTR_H, STR_H})^1$			
Mean	14.2	17.4	3.74
$\Delta_{\%}(\mathbf{qDTR_H})^2$			
Max	10.7	17.4	29.6
Min	-9.4	-16.4	-57.8
$\Delta_{\%}(\mathbf{STR_{RCP}, STR_H})^3$			
2.6	-0.5	-1.3	-0.1
4.5	-0.9	-2.6	-0.2
8.5	-0.5	-3.7	-0.2
$\Delta_{\%}(\mathbf{qDTR_{RCP2.6}, qDTR_H})^3$			
Mean	-0.4	-1.0	-0.1
Max	-1.4	-2.4	-0.5
Min	0.75	0.3	0.8
$\Delta_{\%}(\mathbf{qDTR_{RCP4.5}, qDTR_H})^3$			
Mean	-0.7	-1.7	-0.2
Max	-1.7	-3.2	-0.6
Min	0.9	-0.6	0.5
$\Delta_{\%}(\mathbf{qDTR_{RCP8.5}, qDTR_H})^3$			
Mean	-1.53	-2.3	-0.2
Max	-3.9	-5.1	-1
Min	0.32	-0.8	1.0

[1] The average additional transmission capacity provided by qDTR in place of STR, calculated from historical data.

[2] The spatial variation on the continent of qDTR, calculated from historical data.

[3] The variation of transmission capacity calculated with the specific climatic scenario versus historical weather

The first row shows the spatial variability of $qDTR_H$ in Europe, which is in the region of 20%, 34%, and 87% for OHL, PT, and UGC. As explained above, the lower variability of OHL is due to the double dependency on wind and air temperature of its rating. On the contrary, the very high variability of UGC ratings is due to the variety of soils in the different regions, which considerably impacts thermal diffusivity and moisture retention. The following three rows show the percentage variation in qDTR in Europe according to the different climate scenarios considered. The variations are almost unanimously negative, with peaks in central Spain, the Arctic, and mountainous regions. As mentioned above, UGC presents lower variations because of the high soil inertia.

Finally, the heat map in Fig. 5 represents the temporal variation by month and hour of $qDTR_{RCP}$ on a specific network node. It shows the effect of increasing ambient temperature in the three RCPs scenarios. The observed variations, which are moderately significant, for instance, translate into an average rating reduction of -2.3% in July for $qDTR_{RCP8.5}$ and -0.7% for $qDTR_{RCP4.5}$ in the PT. This could be translated in terms of variation in the risk level regarding the equipment's lifetime for the network operator. On the other hand, the opposite effect can also be observed in specific months and hours, such as -0.9% on February mornings for $qDTR_{RCP8.5}$, +0.7% for $qDTR_{RCP4.5}$ and +0.02% $qDTR_{RCP2.6}$.

3.2 Impact of climate change on network costs

This section examines the G&TEP investment decisions, incorporating climate-variant supply and qDTR for power system components.

To achieve this, we use a network model from the PyPSA [25] package, applying STR_H and $qDTR_{RCP}$ calculated with historical or climate projections using weather data. The network model is then used to carry out a G&TEP to estimate changes in capital expenditure (CAPEX), operational expenditure (OPEX), and renewable curtailment.

The results are summarized in Table 3, which shows:[1] the results of a baseline simulation with STR,[2] the improvements obtained using $qDTR_H$ instead of STR_H, and [3] the error incurred when using historical weather instead of climate projections in $qDTR_{RCP}$ calculations. The expected curtailment amount, the total System Cost, and the LCOE are also reported. However, these values are relative only to new investments and don't consider the existing infrastructure.

Case 1: Reference case, G&TEP for constrained CO2 emissions without considering climate change impact on network transmission capacity. In this case study, the G&TEP model was used to analyze the optimal power system planning and operation under the carbon emission constraints imposed by the RCPs. The model used historical reanalysis data for the STRs. The objective is to

determine the different portfolios of generation capacity necessary to achieve specific emission reduction targets. The study's results are reported in terms of CAPEX and OPEX in billion euros (B€), as well as the renewable curtailment in gigawatt-hours (GWh). The results show that the three scenarios analyzed have virtually the same CAPEX of 355.5 B€ and OPEX of 18.9B€/y, with variations confined to the low percent digits and slightly more visible differences in renewable curtailment. Similar costs nevertheless hide different allocations in the energy mix, with lower investments in Gas power stations in $RCP_{2.6}$ compensated by higher investments in wind. Table 3 reports for this the difference between the results of Case 2 and Case 1.

Case 2: Quantifying the impact on G&TEP of the climate change impact on the transmission network. In this case study, the G&TEP is again calculated for the three RCPs, but with a different set of STRs, estimated using the climatic data from the relative RCPs. The study results are reported in Table 3, which shows the percentage difference for all the parameters between Case 2 and Case 1. The study quantifies how the higher temperatures from climate change, as simulated in the RCPs data, impact the reduced transmission capacity of the network. The results show an increase in CAPEX and a reduction in OPEX, leading to overall higher system costs, except the $RCP_{2.6}$ Scenario.

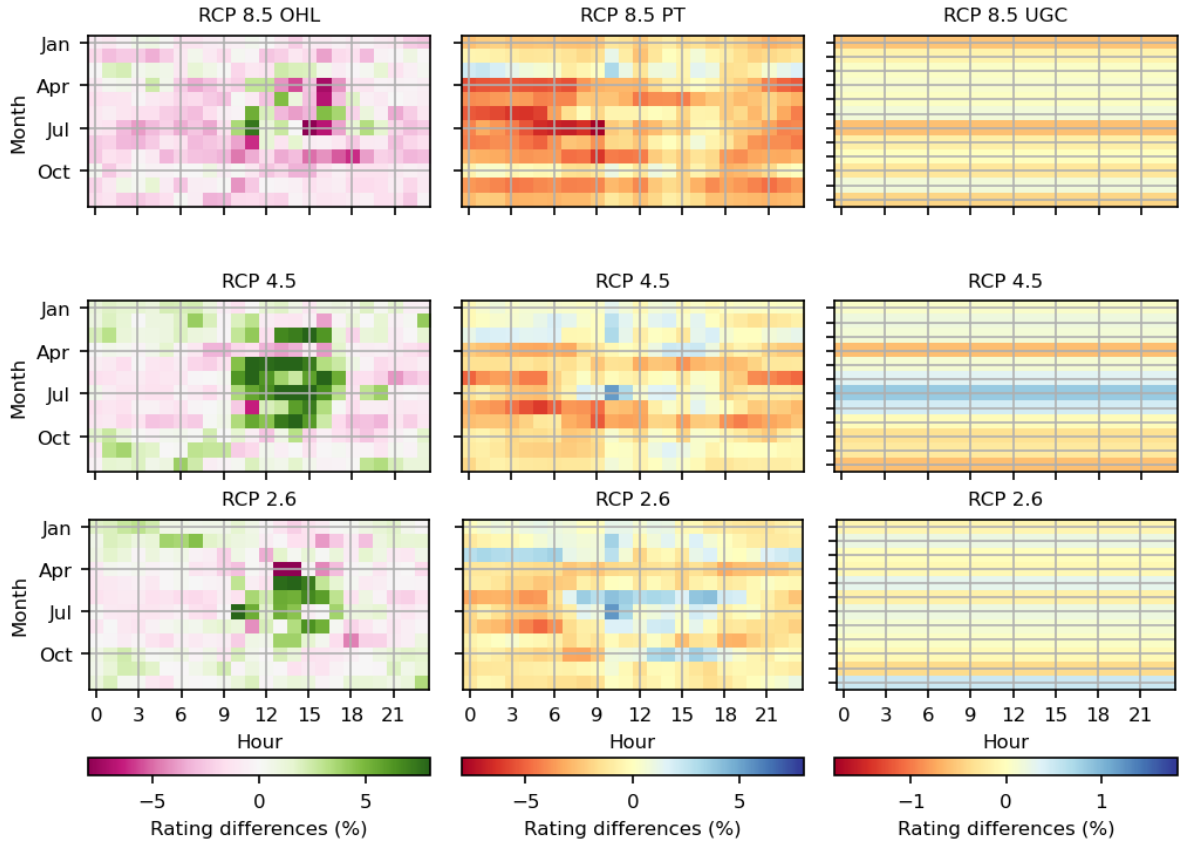

Figure 5: Difference in the calculated qDTR month/hour between historical values and RCP projections 2.6, 4.5, 8.5. This is performed for the three main power components (OHL - PT, and UGC) in a node located in Tavel, southeast France.

Table 3: Variation for the three scenarios concerning yearly fix rating and costs, the scenarios covering historical static (STR_H, historical ($qDTR_H$) and projected ($qDTR_{RCP}$). Values are in % and calculated as 1-y/x, meaning that positive values represent cost reductions and negative values represent cost increases.

SCENARIO		**EUROPE**			**FRANCE**		
RCP		2.6	4.5	8.5	2.6	4.5	8.5
$\mathbf{STR_H}$	CAPEX (B€)	3.55E+2	3.55E+2	3.55E+2	6.65E+1	6.65E+1	6.65E+1
	OPEX(B€)	1.89E+1	1.89E+1	1.89E+1	3.17E+0	3.17E+0	3.17E+0
	System Cost(B€)	4.00E+2	4.00E+2	4.00E+2	7.39E+1	7.39E+1	7.39E+1
	LCOE(€/MWh)	2.77E+1	2.77E+1	2.77E+1	3.53E+1	3.53E+1	3.53E+1
	Curtailment (GW)	7.32E+0	7.30E+0	7.32E+0	1.53E-1	1.54E-1	1.60E-1
$\Delta(\mathbf{STR_{RCP}, STR_H})$	CAPEX (%)	-4.99E-4	-5.16E-3	-1.59E-3	1.12E-3	1.99E-4	-2.37E-3
	OPEX (%)	1.70E-2	4.71E-3	1.26E-2	-6.06E-2	-5.71E-2	-1.66E-2
	System Cost (%)	1.45E-3	-4.06E-3	-7.96E-6	-5.09E-3	-5.57E-3	-3.80E-3
	LCOE(%)	1.45E-3	-4.06E-3	-7.96E-6	-5.09E-3	-5.57E-3	-3.80E-3
	Curtailment (%)	2.57E-1	-5.04E-1	-3.01E-1	6.67E+0	-1.75E+0	9.59E-1
$\Delta(\mathbf{qDTR_H, STR_H})$	CAPEX (%)	2.32E-2	1.42E-2	2.41E-2	1.78E-2	1.51E-2	1.85E-2
	OPEX(%)	1.44E-1	1.36E-1	1.32E-1	-1.87E-1	-1.99E-1	-1.97E-1
	System Cost (%)	3.66E-2	2.77E-2	3.60E-2	-2.73E-3	-6.41E-3	-3.18E-3
	LCOE(%)	3.66E-2	2.77E-2	3.60E-2	-2.73E-3	-6.41E-3	-3.18E-3
	Curtailment (%)	6.49E-1	8.45E-3	4.26E-1	-2.66E-1	5.99E-1	6.77E+0
$\Delta(\mathbf{qDTR_{RCP}\ /\ H})$	CAPEX (%)	-6.26E-3	4.59E+0	-1.20E-2	-2.03E-3	4.75E-3	9.08E-4
	OPEX (%)	4.88E-3	2.20E+1	1.68E-2	1.30E-2	-3.36E-2	5.95E-3
	System Cost (%)	-5.02E-3	6.52E+0	-8.81E-3	-5.19E-4	8.76E-4	1.42E-3
	LCOE(%)	-5.02E-3	6.52E+0	-8.81E-3	-5.19E-4	8.76E-4	1.42E-3
	Curtailment (%)	4.57E-2	4.20E-1	-6.10E-2	-1.20E+0	3.64E+0	-2.13E+0
$\Delta(\mathbf{qDTR_{RCP}, STR_H})$	CAPEX (%)	1.70E-2	4.61E+0	1.21E-2	1.58E-2	1.99E-2	1.94E-2
	OPEX (%)	1.49E-1	2.21E+1	1.49E-1	-1.74E-1	-2.32E-1	-1.91E-1
	System Cost (%)	3.16E-2	6.55E+0	2.72E-2	-3.25E-3	-5.53E-3	-1.76E-3
	LCOE(%)	3.16E-2	6.55E+0	2.72E-2	-3.25E-3	-5.53E-3	-1.76E-3
	Curtailment (%)	6.94E-1	4.28E-1	3.65E-1	-1.47E+0	4.21E+0	4.79E+0

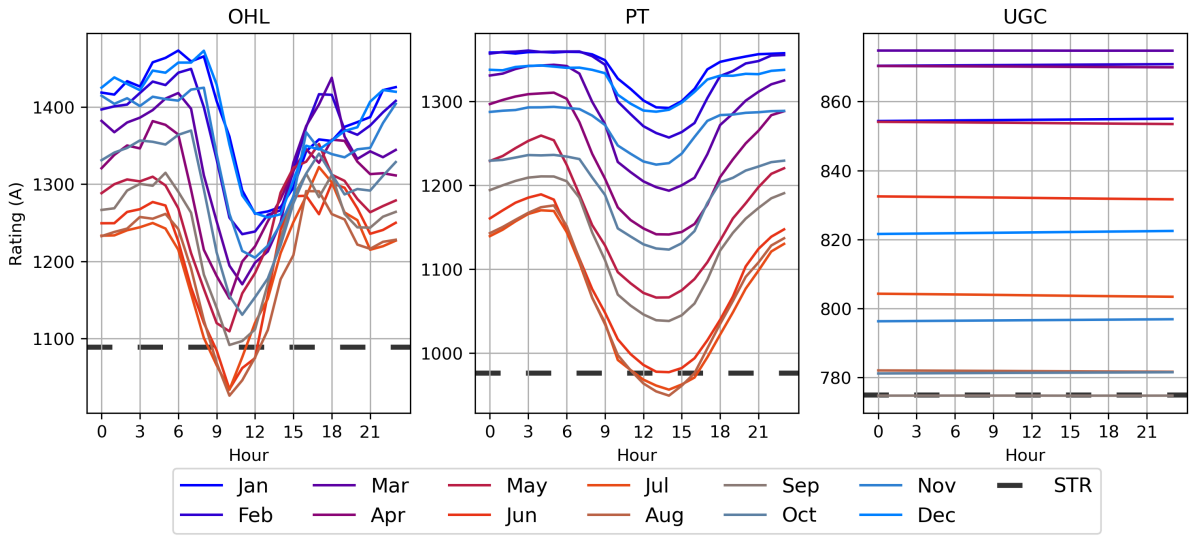

Figure 6: $qDTR_H$ calculated for each month/hour combination for OHL, PT, and UGC calculated in the node of Tavel (southeast France). Colors represent months from the coldest (blue) to the warmest (red). A dashed black line represents yearly static ratings.

3.3 Impact of qDTR vs. STR on network transmission capacity and costs

Case 3: Quantify the benefit of using qDTRs instead of STRs in G&TEP In this use case, the G&TEP is run with a different set of transmission capacity constraints. Instead of using STRs to estimate the available transmission capacity, qDTRs calculated from historical weather reanalysis are used. The objective is to quantify the benefit of qDTRs, mainly due to the exploitation of the higher transmission capacity at night. Results reported in Table 3 show the percentage difference between Case 3 and Case 2 for all the parameters. The results show an overall reduction of costs, both CAPEX and OPEX, in all three scenarios.

Case 4. Quantifying the importance of considering the effect of climate change when calculating qDTRs. In this last use case, the G&TEP model was run considering qDTRs calculated for the respective RCPs. The study's objective is to show the error that would be incurred by not considering the impact of climate change on transmission capacity when using qDTRs. The results, reported in Table 3, show the percentage difference for all the parameters between Case 4 and Case 3. The results show different cost behaviors in the three scenarios, with OPEX and renewable curtailment always underestimated when RCPs are not considered due to the lower effective available transmission capacity.

Finally, the last lines of Table 3 present the cost difference between Case 4 and Case 1. Again, all costs are reduced in all three scenarios, even when higher temperatures and lower transmission capacities are considered.

Fig. 6 shows the yearly and hourly variations of $qDTR_H$ for the three components in southeast France. For OHL and PT, we can see that in daily summer hours, $qDTR_H$ are lower than STR_H. On the contrary, in winter and night hours, $qDTR_H$ are far higher, resulting in a larger overall transmission capacity. Concerning UGC, as expected, their qDTR does not change during the day due to the high thermal inertia of the soil. Another aspect worth mentioning is the daily and yearly variations of $qDTR_H$. For the three components considered, the yearly qDTR variation range in the region is $\pm 15\%$ from the highest to the lowest value, driven by temperature variations.

4 Conclusions

Overall, this work confirms that:

1) Predicted climate, with higher ambient temperatures, causes a reduction in power system transmission capacity in the region of 0.5%, 3,7%, and 0.2% for OHL, PT, and UGL, respectively, in the business as usual RCP8.5 scenario. 2) when this reduction is integrated into a G&TEP study, it results in different combination of CAPEX and OPEX leading to little overall system cost increases for the scenarios $RCP_{8.5}$ and $RCP_{4.5}$, but slightly lower costs in $RCP_{2.6}$.

2) The proposed qDTR approach allows for higher transmission capacities, overcoming the rating reduction caused by climate change. On average, qDTR leads to an increase in transmission capacity in the region of 14.2%, 17.4%, and 3.7% for OHL, PT, and UGC while maintaining a controlled thermal overload probability. This results, in turn, in lower system costs in the three future scenarios and lower renewable curtailment.

Further work: The work must first be carried out on different use cases and more precise network models able to capture better the costs associated to transmission lines. Also, a methodology to better integrate qDTRs within OPF and G&TEP must be developed in order to better understand the limits of this approach.

Furthermore, data and software developed are available for researchers to facilitate the replication and generalization of this study or its use in order to build future research. A sample of this is available for the review period before being uploaded to a more suitable platform at the address: https://minesparis-psl.hal.science/hal-04453957v1

References

[1] "Copernicus Climate Change Service (2021): Climate and energy indicators for Europe from 2005 to 2100 derived from climate projections," Copernicus Climate Change Service (C3S) Climate Data Store (CDS), 2021, accessed on 14-03-2023.

[2] B. B. Hersbach, P. Berrisford, G. Biavati, A. Horányi, J. Muñoz Sabater, Nicolas, C. Peubey, R. Radu, I. Rozum, D. Schepers, A. Simmons, C. Soci, D. Dee, and Thépaut, "ERA5 hourly data on single levels from 1940 to present," 2023, accessed on 14-03-2023.

[3] M. Bartos, M. Chester, N. Johnson, B. Gorman, D. Eisenberg, I. Linkov, and M. Bates, "Impacts of rising air temperatures on electric transmission ampacity and peak electricity load in the united states," *Environmental Research Letters*. [Online]. Available: https://dx.doi.org/10.1088/1748-9326/11/11/114008

[4] S. G. Yalew, M. T. van Vliet, D. E. Gernaat, F. Ludwig, A. Miara, C. Park, E. Byers, E. De Cian, F. Piontek, G. Iyer *et al.*, "Impacts of climate change on energy systems in global and regional scenarios," *Nature Energy*, vol. 5, no. 10, pp. 794–802, 2020.

[5] Y. Romitti and I. Sue Wing, "Heterogeneous climate change impacts on electricity demand in world cities circa mid-century," *Scientific Reports*, vol. 12, p. 4280, 2022. [Online]. Available: https://doi.org/10.1038/s41598-022-07922-w

[6] J. A. Añel, M. Fernández-González, X. Labandeira, X. López-Otero, and L. De la Torre, "Impact of cold waves and heat waves on the energy production sector," *Atmosphere*, vol. 8, no. 11, 2017.

[7] U.S. Department of Energy, "Annual u.s. transmission data review," Tech. Rep., 2018.

[8] "Dynamic thermal rating of transmission lines: A review," *Renewable and Sustainable Energy Reviews*, vol. 91, pp. 600–612, 2018.

[9] B. Keyvani, E. Whelan, E. Doddy, and D. Flynn, "Indirect weather-based approaches for increasing power transfer capabilities of electrical transmission networks," *WIREs Energy and Environment*, vol. 12, no. 3, p. e470.

[10] D. A. Douglass, J. Gentle, H.-M. Nguyen, W. Chisholm, C. Xu, T. Goodwin, H. Chen, S. Nuthalapati, N. Hurst, I. Grant, J. A. Jardini, R. Kluge, P. Traynor, and C. Davis, "A review of dynamic thermal line rating methods with forecasting," *IEEE Transactions on Power Delivery*, vol. 34, no. 6, pp. 2100–2109, 2019.

[11] "Dynamic thermal rating of transmission lines: A review," *Renewable and Sustainable Energy Reviews*, vol. 91, pp. 600–612, 2018.

[12] P. Glaum and F. Hofmann, "Enhancing the german transmission grid through dynamic line rating," in *2022 18th International Conference on the European Energy Market (EEM)*, 2022, pp. 1–7.

[13] A. Trpovski and T. Hamacher, "A comparative analysis of transmission system planning for overhead and underground power systems using ac and dc power flow," in *2019 IEEE PES Innovative Smart Grid Technologies Europe (ISGT-Europe)*, 2019, pp. 1–5.

[14] "Enhancing the hosting capacity of distribution transformers for using dynamic component rating," *International Journal of Electrical Power Energy Systems*, vol. 142, p. 108130, 2022.

[15] "Dynamic rating assists cost-effective expansion of wind farms by utilizing the hidden capacity of transformers," *International Journal of Electrical Power Energy Systems*, vol. 123, p. 106188, 2020.

[16] "Reliability impacts of the dynamic thermal rating and battery energy storage systems on wind-integrated power networks," *Sustainable Energy, Grids and Networks*, vol. 20, p. 100268, 2019.

[17] "Network topology optimisation based on dynamic thermal rating and battery storage systems for improved wind penetration and reliability," *Applied Energy*, vol. 305, p. 117837, 2022.

[18] K. Morozovska, "Dynamic rating with applications to renewable energy," Ph.D. dissertation, KTH Royal Institute of Technology, 2020.

[19] "Forecasting for dynamic line rating," *Renewable and Sustainable Energy Reviews*, vol. 52, pp. 1713–1730, 2015.

[20] D. Douglass, W. Chisholm, G. Davidson, I. Grant, K. Lindsey, M. Lancaster, D. Lawry, T. McCarthy, C. Nascimento, M. Pasha, J. Reding, T. Seppa, J. Toth, and P. Waltz, "Real-time overhead transmission-line monitoring for dynamic rating," *IEEE Transactions on Power Delivery*, vol. 31, no. 3, pp. 921–927, 2016.

[21] M. Mahmoudian Esfahani and G. R. Yousefi, "Real time congestion management in power systems considering quasi-dynamic thermal rating and congestion clearing time," *IEEE Transactions on Industrial Informatics*, vol. 12, no. 2, pp. 745–754, 2016.

[22] I. E. C. (IEC), "Iec 60076-7:2018, power transformers - part 7: Loading guide for mineral-oil-immersed power transformers," International Electrotechnical Commission (IEC), Technical Report, 2018.

[23] I. E. Commission, "Iec 60287-1-1: Electric cables—calculation of the current rating—part 1-1: Current rating equations (100% load factor) and calculation of losses—general," International Electrotechnical Commission, Geneva, Switzerland, Technical Report, 2014.

[24] J. Iglesias, G. Watt, D. Douglass, V. Morgan, R. Stephen, M. Bertinat, D. Muftic, R. Puffer, D. Guery, S. Ueda, K. Bakic, S. Hoffmann, T. Seppa, F. Jakl, C. Do Nascimento, F. Zanellato, and H.-M. Nguyen, *Guide for Thermal Rating Calculations of Overhead Lines*, ser. CIGRE Technical brochure N° 601. CIGRE, December 2014.

[25] T. Brown, D. Schlachtberger, A. Kies, S. Schramm, and M. Greiner, "PyPSA-Eur: An open optimisation model of the european electricity system," *Zenodo*, 2020. [Online]. Available: https://doi.org/10.5281/zenodo.3602442

[26] K. Taylor, R. Stoufer, and G. Meehl, "An overview of cmip5 and the experiment design," *Bull. Am. Meteorol. Soc.*, vol. 93, pp. 485–498, 2011. [Online]. Available: https://doi.org/10.1175/BAMS-D-11-00094.1

[27] "The shared socioeconomic pathways and their energy, land use, and greenhouse gas emissions implications: An overview," *Global Environmental Change*, vol. 42, pp. 153–168, 2017.

[28] F. G. Erdinç, O. Erdinç, R. Yumurtacı, and J. P. S. Catalão, "A comprehensive overview of dynamic line rating combined with other flexibility options from an operational point of view," *Energies*, vol. 13, no. 24, 2020.

[29] C. Matke, W. Medjroubi, and D. Kleinhans, "SciGRID - An Open Source Reference Model for the European Transmission Network (v0.2)," Jul. 2016.

[30] "Comprehensive review of the dynamic thermal rating system for sustainable electrical power systems," *Energy Reports*, vol. 8, pp. 3263–3288, 2022.

[31] R. Olsen, "Dynamic loadability of cable based transmission grids," Ph.D. dissertation, 2013.

[32] A. Bracale, P. Caramia, P. De Falco, A. Michiorri, and A. Russo, "Day-ahead and intraday forecasts of the dynamic line rating for buried cables," *IEEE Access*, vol. 7, pp. 4709–4725, 2019.

[33] "Determining total cost of ownership and peak efficiency index of dynamically rated transformer at the pv-power plant," *Electric Power Systems Research*, vol. 229, p. 110061, 2024.

[34] J. Yang, X. Bai, D. Strickland, L. Jenkins, and A. M. Cross, "Dynamic network rating for low carbon distribution network operation—a u.k. application," *IEEE Transactions on Smart Grid*, vol. 6, no. 2, pp. 988–998, 2015.

[35] Y. Wang, Z. Sun, Z. Yan, L. Liang, F. Song, and Z. Niu, "Power transmission congestion management based on quasi-dynamic thermal rating," *Processes*, vol. 7, no. 5, 2019.

[36] S. Montana and M. Andrea, "Long-term dynamic thermal ratings of underground cables integrating soil dynamics and climate projections."

[37] W. Dorigo and e. a. Himmelbauer, "The international soil moisture network: serving earth system science for over a decade," *Hydrology and Earth System Sciences*, vol. 25, no. 11, pp. 5749–5804, 2021.

[38] R. Hiederer, *Mapping Soil Properties for Europe - Spatial Representation of Soil Database Attributes*, ser. EUR26082EN Scientific and Technical Research. Luxembourg: Publications Office of the European Union, 2013.

[39] E. Kiessling, P. Nefzger, J. Nolasco, and U. Kaintzyk, *Overhead Power Lines Planning, Design, Construction – Hard-drawn AL1 ACSR*, edition ed. City: PublisherName, 2019.

[40] T.-F. K. S.A., *High and extra high voltage cables*, edition ed. City: www.tfkable.com, 2019.

[41] 529 Working Group A2.36, "Guidelines for conducting design reviews for power transformers," Publisher Name, Technical Report Report Number, April 2013.

[42] G. J. Anders, *Rating of electric power cables in unfavorable thermal environment*, 2005.

[43] B. Gorgan, P. V. Notingher, J. M. Wetzer, H. F. Verhaart, P. A. Wouters, and A. V. Schijndel, "Influence of solar irradiation on power transformer thermal balance," *IEEE Transactions on Dielectrics and Electrical Insulation*, vol. 19, no. 6, pp. 1843–1850, 2012.

[44] T. Brown, J. Hörsch, and D. Schlachtberger, "PyPSA: Python for Power System Analysis," *Journal of Open Research Software*, vol. 6, no. 4, 2018. [Online]. Available: https://doi.org/10.5334/jors.188

[45] D. van Vuuren, M. den Elzen, P. Lucas, B. Eickhout, B. Strengers, B. van Ruijven, S. Wonink, and R. van Houdt, "Stabilizing greenhouse gas concentrations at low levels: an assessment of reduction strategies and costs," *Climatic Change*, 2007.

[46] L. Clarke, J. Edmonds, H. Jacoby, H. Pitcher, J. Reilly, and R. Richels, "Scenarios of greenhouse gas emissions and atmospheric concentrations," U.S. Climate Change Science Program and the Subcommittee on Global Change Research, Department of Energy, Office of Biological & Environmental Research, Washington, DC, USA, Sub-report 2.1A of Synthesis and Assessment Product 2.1, 2007.

[47] S. Smith and T. Wigley, "Multi-gas forcing stabilization with the minicam," *Energy Journal (Special Issue 3)*, pp. 373–391, 2006.

[48] M. Wise, K. Calvin, A. Thomson, L. Clarke, B. Bond-Lamberty, R. Sands, S. Smith, A. Janetos, and J. Edmonds, "Implications of limiting co2 concentrations for land use and energy," *Science*, vol. 324, pp. 1183–1186, May 29 2009.

[49] J. Fujino, R. Nair, M. Kainuma, T. Masui, and Y. Matsuoka, "Multi-gas mitigation analysis on stabilization scenarios using aim global model," *Multigas Mitigation and Climate Policy. The Energy Journal Special Issue*, 2006.

[50] Y. Hijioka, Y. Matsuoka, H. Nishimoto, M. Masui, and M. Kainuma, "Global ghg emissions scenarios under ghg concentration stabilization targets," *Journal of Global Environmental Engineering*, vol. 13, pp. 97–108, 2008.

[51] K. Riahi, A. Gruebler, and N. Nakicenovic, "Scenarios of long-term socio-economic and environmental development under climate stabilization," *Technological Forecasting and Social Change*, vol. 74, no. 7, pp. 887–935, 2007.